Impulse TDR and its Application to Measurement of Antennas

Steven McCabe[1], Jonathan Scott[2]

Department of Engineering, The University of Waikato,
Gate 8 Hillcrest Road, Hamilton, New Zealand
[1]som1@waikato.ac.nz
[2]jonathanscott@ieee.org

***Abstract*—The traditional stimulus signal used in a time-domain reflectometer (TDR) is a voltage step. We propose an alternative technique, whereby an impulse generator is employed in place of the step generator in a TDR. The advantage conferred by "impulse TDR" is that more energy is available at higher frequencies than with conventional step TDR, and so a higher bandwidth and signal-to-noise ratio (SNR) is achieved. The theoretical result is compared with measurement.**

***Index Terms*—Antenna measurements, frequency-domain (FD) analysis, pulse measurements, time domain reflectometry (TDR), transient response.**

I. Introduction

Time-domain reflectometry (TDR) is a well-known technique that is typically used to measure the impedance of discontinuities as a function of time (or distance) in electronic systems [1]–[4]. A TDR instrument consists primarily of an oscilloscope and a test signal generator, where the test signal is traditionally a voltage step. As a consequence of the Fourier transform, the energy in the spectrum of a step falls with increasing frequency. On the other hand, an ideal impulse (Dirac delta) test signal has a theoretically flat bandwidth. In this paper, we explore the advantages of making impulse TDR measurements, similar to a traditional step TDR but employing an impulse-like signal instead of a step-like signal. The work is timely because a high-quality impulse generator has recently become commercially available [5]–[7]. This allows us to compare theory with measurement.

II. Time-Domain Comparisons Between Step TDR and Impulse TDR

Fig. 1 illustrates a variety of different waveforms for common load conditions on a characteristic line impedance, Z_0, in the well-known case of a TDR built using a step stimulus signal, compared with the case of an impulse stimulus signal. The waveforms contain the incident stimulus signal that is applied to the load impedance, Z_L, followed by some signal reflected back to the TDR. The middle column of the figure will be familiar to many practitioners. The waveforms that result from the various load circuits are "common sense" and easily remembered or worked out with some familiarity. However, the waveforms in the right-hand column, in the case of the impulse signal, are neither familiar nor obvious. This difference arises because the emphasis of energy on low frequencies in the step case results in waveforms that resemble the classic transient response waveforms for RC and RL circuits that are taught in junior circuit theory courses. No such familiar resemblance arises in the impulse case. For this reason, impulse TDR is not likely to replace step TDR in the analysis of simple discontinuities on a transmission line.

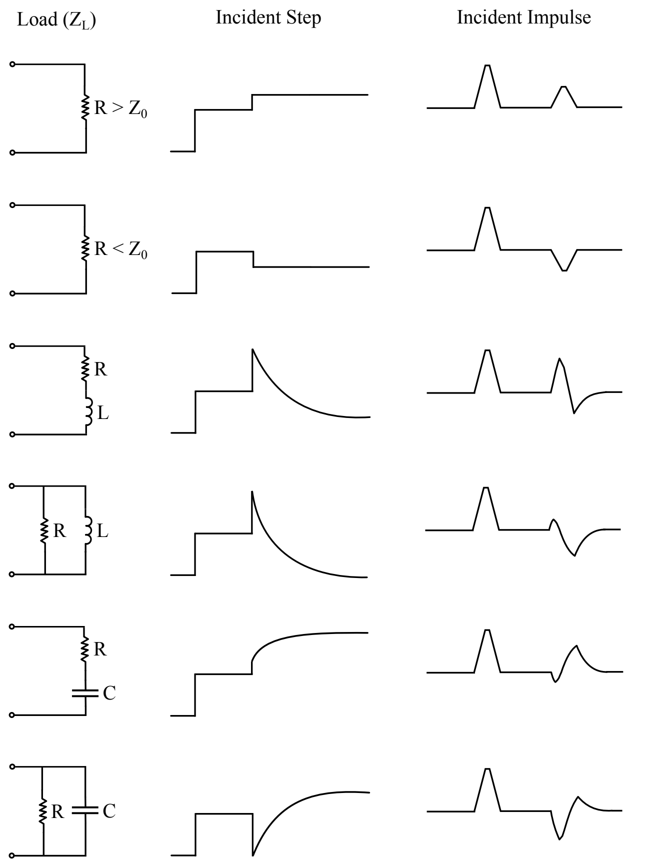

Fig. 1. Comparison of visual displays to be expected for a variety of common load circuits in the case of conventional step TDR and the proposed impulse TDR.

III. Fourier Transform of the Stimulus Signal

The unit impulse (Dirac delta) function is defined as having zero amplitude for all time except at $t = 0$, where it has infinite amplitude:

$$\delta(t) = \begin{cases} 0, & t \neq 0 \\ \infty, & t = 0 \end{cases}$$

The Fourier transform for the unit impulse is

$$\mathrm{F}[\delta(t)] = 1 \tag{1}$$

Therefore, an ideal impulse has a flat frequency response. Although the unit impulse is a theoretical construct and cannot physically exist [8], it is used as a limiting case for when the width of a pulse approaches zero. Derived from the convolution of two rectangular ("rect") functions, the trapezoid function provides an approximation of a realistic impulse with finite rise and fall times [9]:

$$u(t) = \frac{1}{\tau}\,\mathrm{rect}\left(\frac{t}{\tau}\right) \otimes A\,\mathrm{rect}\left(\frac{t}{T}\right) \tag{2}$$

where A is the trapezoid amplitude, T is the full width at half maximum (FWHM), and τ is the rise/fall time from 0 to 100% of the amplitude. The Fourier transform of $u(t)$ is given by

$$\mathrm{F}[u(t)] = AT\,\mathrm{sinc}(f\tau)\,\mathrm{sinc}(fT) \tag{3}$$

The Heaviside unit step function is defined as

$$H(t) = \begin{cases} 1, & t > 0 \\ \frac{1}{2}, & t = 0 \\ 0, & t < 0 \end{cases}$$

This function represents an ideal voltage step which is immediately elevated to a constant level at a definite time [10]. The Fourier transform of $H(t)$ is given by

$$\mathrm{F}[H(t)] = \frac{1}{j2\pi f} + \frac{1}{2}\delta(f) \tag{4}$$

The response varies as the reciprocal of frequency and so approaches zero magnitude as frequency tends to infinity. This theoretical construct cannot physically exist as a realistic step waveform has a finite rise time. The Fourier transform for a step function $s(t)$ with finite rise time is given by

$$\mathrm{F}[s(t)] = A\frac{1}{j2\pi f}\,\mathrm{sinc}(f\tau) \tag{5}$$

where τ is the rise time from 0 to 100% of the amplitude A.

Fig. 2 presents a number of spectra that will be compared with the spectrum of an ideal step (Heaviside unit step) that appears as the dashed line. The new impulse source generates impulses with a typical FWHM of 23 ps [11]. The rise/fall time is estimated as 18 ps (5 ps flat-top). By inserting these parameters in (3), the Fourier transform of a unit amplitude impulse with finite rise and fall times was simulated in Matlab. This can now be compared with the spectrum for the Heaviside unit step from (4) and some realistic step waveforms from (5) in Fig. 2. It can be seen that even the realistic, limited impulse signal contains more energy than an ideal step for frequencies above about 7.5 GHz. When the step waveform is not ideal, but similar to what is practically available today, the comparison becomes even more favorable, as can be seen in the same figure.

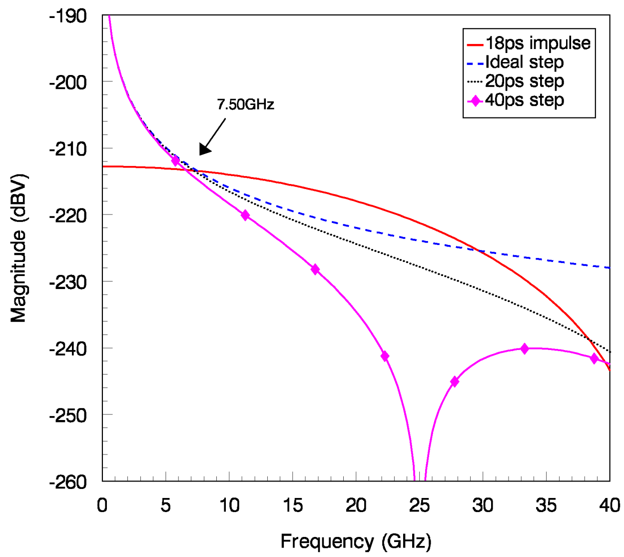

Fig. 2. The Fourier transforms of an ideal unit step, some practical step-like signals, and a practical trapezoidal pulse of unit amplitude. The unit for magnitude is dBV, namely the voltage relative to 1 Volt.

IV. Step TDR and Impulse TDR Measurements of an Antenna

Recent studies have demonstrated the successful use of step TDR to characterise the reflection scattering parameter $S_{11}(f)$ of antennas [12], [13]. The motivation behind this work is driven by the fact that a TDR is less expensive than a vector network analyser (VNA), but more importantly the time-localisation of the energy in the transient test signal means that the user can dispense with the anechoic chamber that is required for antenna measurements with a sinewave exciting signal. Subsequent sections describe the measurement of an antenna using the proposed impulse TDR and compare with measurements obtained using conventional step TDR and VNA methods.

A. Measurement System

An impulse-style TDR was constructed as shown in Fig. 3. The set-up features an Agilent U9391C impulse generator, an Agilent 11636B divider, an Agilent 54754A TDR module, and an Agilent 86100C mainframe in oscilloscope mode. The device under test (DUT) was a Laird Technologies SAH58-120-16-WB wideband sector antenna. The antenna was designed to operate within the 5.47-5.85 GHz frequency range.

The impulse generator produces a series of impulses that are split between the DUT and oscilloscope via a resistive divider. The temporal spacing between each impulse is set by the frequency of the RF source and the generator's internal frequency divider [11]. When an impulse arrives at the DUT, unless the DUT has an impedance equivalent to the characteristic impedance of the system, the DUT will reflect a voltage signal back toward the resistive divider and into the oscilloscope to be measured. Due to high bandwidth requirements, an equivalent-time sampling oscilloscope is employed where triggering is supplied by an external signal from the impulse generator.

A step-type TDR set-up was constructed using a similar configuration but with the impulse source replaced with a 50Ω dummy load and the mainframe set in TDR mode. The divider was included to allow for fair comparison between the impulse

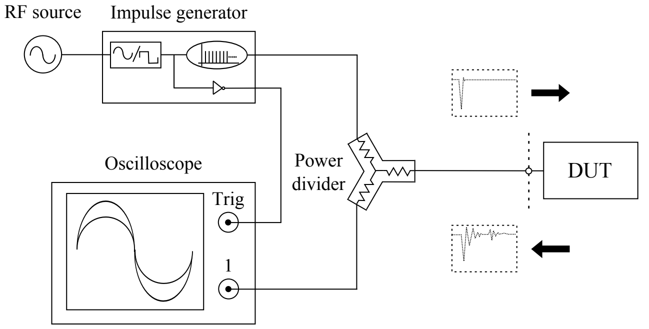

Fig. 3. The set-up for impulse TDR measurements. The dashed line represents the reference plane at the DUT connector.

TDR and step TDR techniques. An attenuator was also inserted between the oscilloscope channel and the divider, to further reduce the step signal to a similar amplitude produced in the impulse TDR set-up.

Calibrated measurements were acquired using a VNA, where the DUT was situated outdoors to provide an accurate reference for comparison with the TDR measurements.

B. Acquisition in the Time-Domain

Two time-domain measurements were employed in the subsequent frequency-domain processing: A reference waveform reflected from a short-circuit, and the waveform reflected by the antenna. Averaged measurements taken by the impulse TDR set-up were windowed with the Dirichlet window in Matlab, to remove the incident portion of the signal and to remove spurious reflections as required for subsequent frequency-domain processing as reported in [12]. The rectangular window contained the essential data that corresponded to the DUT response, and provided a reference plane extended to the end of the cable where the DUT was to be attached. The length of the time window was chosen so that there was sufficient time for the antenna's reflection to settle, while limited to block out spurious reflections caused by the presence of objects near the antenna. Initially, a $35\,\mathrm{ns}$ acquisition window was chosen as endorsed in [12].

Shown in Fig. 4(a) is the reference waveform derived from a short-circuit connected at the reference plane. The large spike corresponds to the reflected impulse, followed by some oscillatory behaviour characteristic of the short-circuit. The short-circuit was replaced with the wideband antenna, and its reflection was measured as shown in Fig. 4(b). The first peak corresponds to the mismatch between the transmission line and the antenna connector. A feed cable within the antenna housing introduced a small delay prior to the actual antenna reflection. The next portion of the waveform corresponds to the resonant behaviour of the antenna. It is clear the $35\,\mathrm{ns}$ acquisition window was sufficient in length as the waveform approaches a steady-state condition before the window ends.

The same process was followed for the acquisition of the step-type TDR measurements.

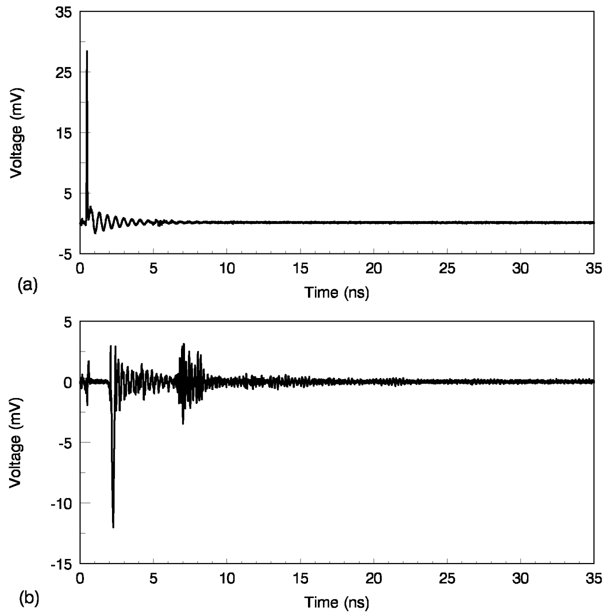

Fig. 4. Plot of the reflected signal seen by the impulse TDR when the (a) short-circuit is connected at the reference plane (b) wideband antenna is connected at the reference plane.

C. Transformation to the Frequency-Domain

Prior to frequency-domain transformation, the time-domain data was processed with the Nicolson algorithm to avoid truncation errors along with the zero-padding operation to ensure adequate frequency resolution [14]. A computer program computed the discrete Fourier transform (DFT) for both the reference reflection and DUT reflection, resulting in $V_{ref}(f)$ and $V_{DUT}(f)$. The reflection scattering parameter $S_{11}(f)$ was then computed by $S_{11}(f) = V_{DUT}(f)/V_{ref}(f)$ for frequencies between 5.4-$6.2\,\mathrm{GHz}$. The DUT $|S_{11}(f)|_{\mathrm{dB}}$ response obtained by both the impulse TDR and step TDR methods, were plotted against the VNA reference as shown in Fig. 5. The frequency range shown is constrained to the antenna's specified operating range. The root mean square error (RMSE) between the VNA and impulse TDR $|S_{11}(f)|$ measurements was calculated as 0.027, whereas the RMSE between the VNA and step TDR $|S_{11}(f)|$ measurements was 0.073. Therefore, the impulse TDR measurement follows the VNA reference more closely than does the step TDR measurement.

D. Dynamic Range

The spectra measured in the reflection from a short-circuit for both the impulse TDR and step TDR systems is shown in Fig. 6(a). Similarly, the spectra present in the DUT reflection for each TDR set-up is shown in Fig. 6(b). It is apparent from both figures that the energy in the impulse TDR reflection exceeds the energy in the step TDR reflection above about $3.1\,\mathrm{GHz}$. Beyond $3.1\,\mathrm{GHz}$ the $23\,\mathrm{ps}$ impulse TDR offers a significant improvement in SNR compared with the Agilent 54754A $40\,\mathrm{ps}$ step TDR. It is worth mentioning that the DFT treats the time-domain waveforms as periodic, resulting in

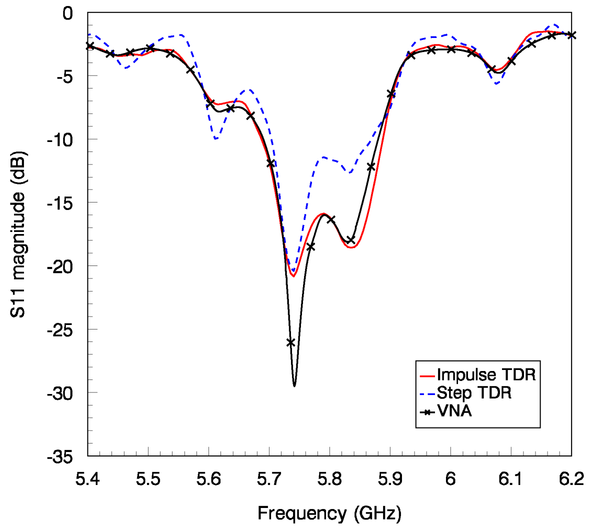

Fig. 5. Comparison of $|S_{11}(f)|_{\text{dB}}$ measurements made by the impulse TDR, step TDR, and VNA, limited to the working frequency range of the wideband antenna.

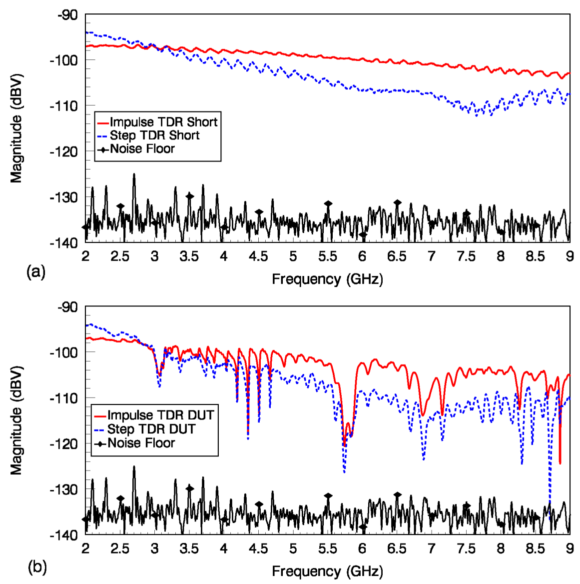

Fig. 6. The frequency spectra for the impulse TDR and step TDR measurements when the (a) reference short-circuit was connected at the reference plane (b) DUT was connected at the reference plane. The noise floor was determined by measuring the noise present in the system with the signal source disabled.

spectra that are scaled slightly different in magnitude than the spectra produced by the continuous Fourier transform of single transient signals in Fig. 2.

Recommendations for the application of impulse TDR, step TDR, and VNA measurement techniques, are summarised in Table I.

V. Conclusion

Impulse TDR does not have an intuitive or informative display, making it less desirable for conventional measurements. However, in the situation where the user will post-process reflection waveform data, for example, to determine S-parameters, the impulse version of TDR is superior at frequencies above 7.5 GHz. It may also be advantageous when the user is looking for precision in spatial localisation, say in a connector or similar in-line structure, as the increased energy at higher frequencies can help.

TABLE I
Comparison of Measurement Techniques

Technique	Bandwidth	Dynamic range	Equipment cost	Anechoic chamber
Impulse TDR	Med	Med	Med	No
Step TDR	Low	Low	Med	No
VNA	High	High	High	Yes

Acknowledgement

The authors wish to acknowledge the support of Agilent Technologies Component Test Division for the supply and detailed support of equipment. Thanks are also due to Skynet Data Communications Technology Ltd for the supply of equipment and support.

References

[1] *Time Domain Reflectometry Theory,* Agilent Technologies, USA, Application Note 1304-2, 2006. http://cp.literature.agilent.com/litweb/pdf/5966-4855E.pdf retrieved Jan 2010.

[2] M. Harper, N. Ridler, and M. Salter, “Comparison Between Root-Impulse-Energy and Vector Network Analyzer Methods for Measuring Loss on Printed Circuit Boards”, in *ARFTG Microwave Measurement Symp.*, in Portland, OR, 2008, pp. 20-25.

[3] C. Chiu, W. Chen, K. Liao, B. Chen, Y. Teng, G. Huang, and L. Wu, “Pad Characterization for CMOS Technology Using Time Domain Reflectometry”, in *Proc. IEEE Int. RF and Microwave Conf.*, in Kuala Lumpur, Dec. 2008, pp. 215-217.

[4] H. Songoro, M. Vogel, and Z. Cendes, “Keeping Time with Maxwell’s Equations”, *IEEE Microwave Magazine*, vol. 11, no. 2, pp. 42-49, Apr. 2010.

[5] J. Scott and D. Gunyan, “Pulse Generator”, US patent number *7,423,470*, Sep, 2008.

[6] J. Scott and M. Hoy, “Group-Delay Measurement of Frequency-Converting Devices Using a Comb Generator”, *IEEE Trans. Instrum. Meas.*, vol. 59, no. 11, pp. 3012-3017, Nov. 2010.

[7] P. Blockley, D. Gunyan, and J. Scott, “Mixer-Based, Vector-Corrected, Vector/Network Analyzer Offering 300kHz-20GHz Bandwidth and Traceable Response”, *IEEE Int. Microwave Symp.* in Long Beach, CA, Jun. 2005, pp. 1-4.

[8] S. Haykin and M. Moher, “Introduction to Analog & Digital Communications, Second Edition”, *John Wiley & Sons, Inc*, pp. 42-49, 2007.

[9] D. Brandwood, “Fourier Transforms in Radar and Signal Processing”, *Artech House, Inc.*, pp. 39-47, 2003.

[10] R. N. Bracewell, “The Fourier Transform and its Applications, Third Edition”, *McGraw-Hill International Editions*, pp. 61, 2000.

[11] “Agilent U9391C/F Comb Generators Technical Overview”, *Agilent Technologies*, http://www.home.agilent.com/agilent/product.jspx?pn=U9391C retrieved Jan 2010.

[12] A. Cataldo, G. Monti, E. De Benedetto, G. Cannazza, L. Tarricone, and L. Catarinucci, “Assessment of a TD-Based Method for Characterization of Antennas”, *IEEE Trans. Instrum. Meas.*, vol. 58, no. 5, pp. 1412-1419, May. 2009.

[13] R. Tamas, G. Caruntu, and D. Popa, “A Time-Domain Measuring Technique for Ultra-Wide Band Antennas”, *Microwave and Optical Technology Letters*, vol. 53, no. 2, pp. 281-286, Feb. 2011.

[14] A. Cataldo, L. Catarinucci, L. Tarricone , F. Attivissimo, and A. Trotta, “A TD-FD Combined Method for Enhancing Reflectometry Measurements in Liquid Quality Monitoring”, in *Proc. IEEE Instrum. Meas. Tech. Conf.*, in Warsaw, May. 2007, pp. 1-5.